ROS

RESEARCH ARTICLES

Nrf2 Deficiency Promotes Melanoma Growth and Lung Metastasis

Hong Zhu[1], Zhenquan Jia[2], Michael A. Trush[3], and Y. Robert Li[1,2,4,5]

[1]Campbell University Jerry M. Wallace School of Osteopathic Medicine, Buies Creek, NC 27506, USA; [2]Department of Biology, University of North Carolina, Greensboro, NC 27412, USA; [3]Department of Environmental Health Sciences, The Johns Hopkins University Bloomberg School of Public Health, Baltimore, MD 21205, USA; [4]Virginia Tech-Wake Forest University School of Biomedical Engineering and Sciences, Blacksburg, VA 24061, USA; [5]Department of Biomedical Sciences and Pathobiology, Virginia Polytechnic Institute and State University, Blacksburg, VA 24061, USA

Correspondence: zhu@campbell.edu (H.Z.)

Zhu H et al. Reactive Oxygen Species 2(4):308–314, 2016; ©2016 Cell Med Press
http://dx.doi.org/10.20455/ros.2016.853
(Received: May 18, 2016; Revised: May 27, 2016; Accepted: May 28, 2016)

ABSTRACT | The role of Nrf2, a key regulator of antioxidant and cytoprotective genes, in tumorigenesis remains controversial. Here we showed that Nrf2 deficiency led to increased local tumor growth in mice following subcutaneous injection of B16-F10 melanoma cells, as indicated by increased proportion of animals with locally palpable tumor mass and time-dependent increases in tumor volume at the injection site. In vivo bioluminescence imaging also revealed increased growth of melanoma in Nrf2-null mice as compared with wild-type mice. By using a highly sensitive bioluminometric assay, we further found that Nrf2 deficiency resulted in a remarkable increase in lung metastasis of B16-F10 melanoma cells as compared with wild-type mice. Taken together, the results of this short communication for the first time demonstrated that Nrf2 deficiency promoted melanoma growth and lung metastasis following subcutaneous inoculation of B16-F10 cells in mice.

KEYWORDS | B16-F10 cells; Bioluminescence imaging; Bioluminometry; Lung metastasis; Melanoma; Nrf2

ABBREVIATIONS | ATP, adenosine triphosphate; DMEM, Dulbecco's modified Eagle's medium; FBS, fetal bovine serum; Nrf2, nuclear factor E-2 related factor 2; PBS, phosphate-buffered saline; ROS, reactive oxygen species

CONTENTS

1. INTRODUCTION

The nuclear factor E-2 related factor 2 (Nrf2) is best known as the chief regulator of antioxidant, anti-inflammatory, and cytoprotective genes, including those encoding phase 2 enzymes that are involved in detoxifying many chemical carcinogens [1]. In this context, Nrf2 signaling was shown to play an important role in protecting against chemical carcinogenesis in a number of animal models [1–3]. In contrary, sustained activation of Nrf2 via genetic and/or other approaches was found to promote spontaneous carcinogenesis in multiple animal models [4–6]. It has been thus suggested that Nrf2 signaling may protect against cancer cell initiation by chemical carcinogens, but promote tumorigenesis once the initiation occurs. However, this notion was not supported by studies showing that targeted deletion of Nrf2 reduced urethane-induced lung tumor development in mice [7] and that Nrf2 knockout enhanced intestinal tumorigenesis in $Apc^{min/+}$ mice due to attenuation of anti-oxidative stress pathway [8]. Hence, the exact role of Nrf2 signaling in tumorigenesis remains controversial and appears to be influenced by diverse factors, including the type of chemical carcinogens and the type of cancers as well as the physiological and pathophysiological conditions of the host. To further investigate the role of Nrf2 in tumorigenesis, in this study, we determined the impact of Nrf2 deficiency on local growth and lung metastasis of melanoma following subcutaneous inoculation of B16-F10 melanoma cells in mice.

2. MATERIALS AND METHODS

2.1. Materials

The luciferase-expressing B16-F10 melanoma (B16-F10-luc-G5 Bioware® Ultra) cells and luciferin were obtained from PerkinElmer (Waltham, MA). Dulbecco's modified Eagle's medium (DMEM), penicillin, streptomycin, fungizone, fetal bovine serum (FBS), zeocin, and phosphate-buffered saline (PBS) were from Thermo Fisher Scientific (Grand Island, NY). Cell culture flasks and other plasticwares were from Corning (Corning, NY). Adenosine triphosphate (ATP) and other chemicals and reagents of analytical grade were purchased from Sigma-Aldrich (St. Louis, MO).

2.2. Cell Culture and Sample Preparation

The B16-F10-luc-G5 cells were cultured in DMEM supplemented with 10% FBS, 100 units/ml of penicillin, 100 μg/ml of streptomycin, and 0.25 μg/ml of fungizone at 37°C in a humidified atmosphere of 5% CO_2. For zeocin selection, the B16-F10-luc-G5 cells were cultured in the above medium in the presence of zeocin (0.25 mg/ml) for 1 week. For cell homogenate preparation, a known number of the cells were lysed in 25 mM phosphate buffer (pH 7.8) containing 2 mM ethylenediaminetetraacetic acid (EDTA), 2 mM $MgSO_4$, and 0.1% Triton X-100, and the cell lysate was kept on ice for bioluminescence measurement within 2 hours or stored at –90°C for subsequent measurement within 2 months.

2.3. Animals and Treatment

Nrf2-null C57BL/6 mice were obtained from Jackson Laboratory (Bar Harbor, ME). Male Nrf2-null and wild-type mice at the age of 7–8 weeks were used in the experiments. These mice were housed in an institutional animal research facility with a light period from 6 am to 6 pm. Purified AIN-93G chow (BioServ, NJ) and water were available ad libitum. All mice were allowed to acclimate for at least one week prior to the experiments.

For studying melanoma growth and lung metastasis, each of the Nrf2-null (n = 11) and wild-type (n = 10) mice was injected subcutaneously with 1×10^6 B16-F10 cells in 0.1 ml phosphate buffered saline on day 0, and the body weight and tumor size were

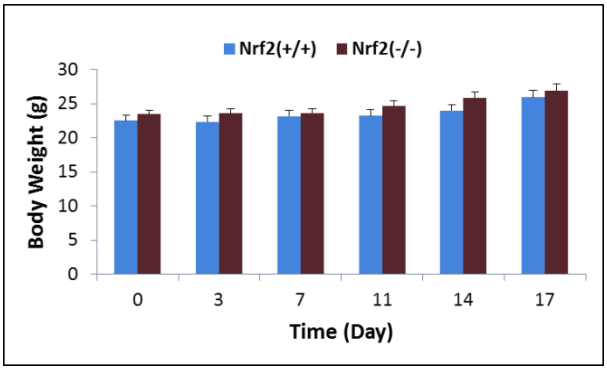

Figure 1. Changes of body weight between Nrf2-null and wild-type mice at the different time points following subcutaneous inoculation of B16-F10 cells. Data represent means ± SEM (n = 11 for Nrf2-null group and n = 10 for wild-type group).

measured at days 3, 7, 11, 14, and 17. The tumor size at the injection site was estimated by measuring the width, length, and height of the tumor mass using a caliper, and the volume was calculated using the formula of volume = 0.5 × (width × length × height) with the unit being cm^3. On day 17, all mice were euthanized, and the lungs were collected for examination of surface foci formed by B16-F10 melanoma cell metastasis. After photographing, the entire lungs were homogenized in 1 ml of 25 mM phosphate buffer (pH 7.8) containing 2 mM EDTA, 2 mM MgSO4, and 0.1% Triton X-100, and the homogenates were kept on ice for bioluminescence measurement. The animal procedures were approved by the Institutional Animal Care and Use Committee in compliance with the pertinent U.S. Federal policy.

2.4. In Vivo Bioluminescence Imaging

The in vivo imaging experiment was performed with a Berthold Night Owl LB 981imaging system (Wildbad, Germany) following subcutaneous infusion of luciferin (100 µg/ml) and ATP (0.5 mM) in a volume of 50 µl at the site of the initial injection of B16-F10 cells in both Nrf2-null and wild-type mice. The images were acquired at room temperature for 5 min and analyzed using the WinLight32 software. The final tumor images were created by overlaying the bioluminescence images on top of the photos of the respective animals.

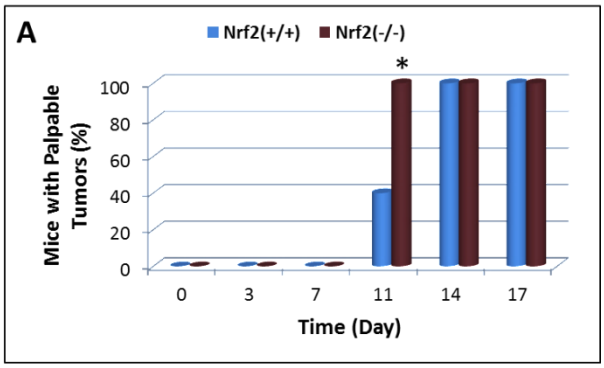

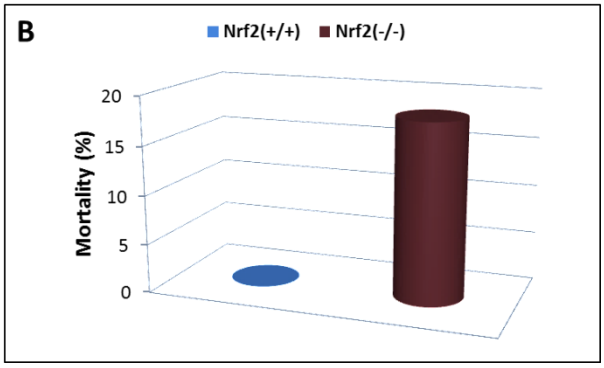

Figure 2. Proportion of mice with palpable tumor mass at the different time points (panel A) and mortality at day 17 (panel B) in Nrf2-null and wild-type mice following subcutaneous inoculation of B16-F10 cells. n = 11 for Nrf2-null group and n = 10 for wild-type group. *, $p < 0.05$ compared with respective wild-type group.

2.5. Bioluminometric Quantification of Melanoma Cell Load in the Lungs

Bioluminescence was measured with a Berthold multi-channel LB 9505C luminometer (Wildbad, Germany) at 37°C for 5 min in a clear plastic tube filled with 1 ml of 25 mM phosphate buffer (pH 7.8) containing 2 mM EDTA, 2 mM MgSO4, and 0.1% Triton X-100, in the presence of luciferin (100 µg/ml) and ATP (0.5 mM). The reaction was started by adding cell or tissue samples to the above reaction mix. The luciferase/luciferin-derived bioluminescence intensity was expressed as integrated responses (total counts of photon emission) over the above 5 min. The melanoma cell load per mouse lungs was deter

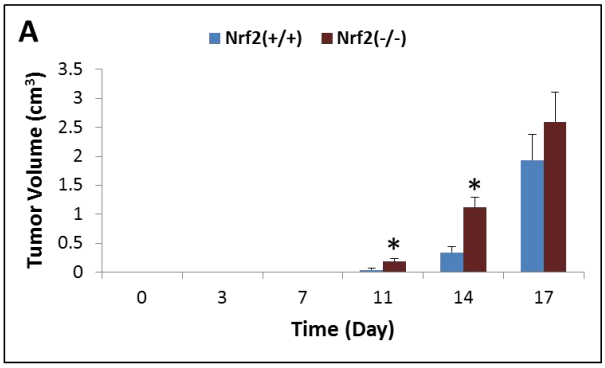

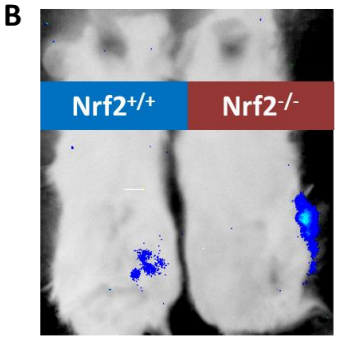

Figure 3. Time-dependent increases in tumor volume (panel A) and a representative in vivo bioluminescence image of tumor growth (panel B) at the site of injection in Nrf2-null and wild-type mice following subcutaneous inoculation of B16-F10 cells. Data in panel A represent means ± SEM (n = 11 for Nrf2-null group and n = 10 for wild-type group). *, $p < 0.05$ compared with respective wild-type group.

mined by using a concurrently run standard curve of known numbers of B16-F10 cells as described previously [9].

2.6. Statistical Analyses

All data are expressed as means ± SEM with an n of 10 or 11 unless otherwise indicated. Differences between the mean values of the Nrf2-null and wild-type mice were analyzed by the *t*-test. The percentage (proportion) differences between Nrf2-null and wild-type mice were analyzed by the chi-square test. Statistical significance was considered at $p < 0.05$.

3. RESULTS

3.1. Nrf2 Deficiency and Melanoma Growth

The body weight changes between Nrf2-null and wild-type mice during the period of the experiment were not significantly different. The body weigh was increased by 14.6% and 15.5% between day 0 and day 17 in Nrf2-null and wild-type mice, respectively (**Figure 1**). Between day 0 and day 7, no palpable tumor mass was noticed in either Nrf2-null or wild-type mice. However, on day 11, all of the 11 Nrf2-null mice had palpable tumor mass at the injection site, whereas only 4 out of the 10 wild-type mice had palpable tumor mass ($p < 0.05$). All wild-type mice along with the Nrf2-null mice had palpable tumor mass on days 14 and 17 (**Figure 2A**). On day 17, 2 of the 11 Nrf2-null mice were dead and none in the wild-type group was dead (**Figure 2B**), but this difference was not statistically significant ($p > 0.05$).

In both Nrf2-null and wild-type mice the tumor volume increased remarkably between day 11 and day 17 (**Figure 3A**). The volume of tumor mass at the injection site in Nrf2-null mice was 4.1 and 3.3 times larger than that in wild-type mice on day 11 and day 14, respectively ($p < 0.05$). There was no statistical difference in tumor volume between Nrf2-null and wild-type mice on day 17 (**Figure 3A**). In vivo bioluminescence imaging also showed a remarkable increase in tumor growth in Nrf2-null mice as compared with wild-type mice on days 11 and 14. A representative in vivo image on day 11 was shown in **Figure 3B**.

3.2. Nrf2 Deficiency and Lung Metastasis

All mice from both Nrf2-null and wild-type groups were euthanized on day 17 for examination of lung foci, and none showed the formation of surface foci of B16-F10 cells (data not shown). Quantification of the total melanoma cell load in the mouse lungs was performed using a highly sensitive bioluminometric assay based on a concurrently run standard curve (**Figure 4A**). As shown in **Figure 4B**, the mean melanoma cell load per mouse lungs was 30,788 and 1,570 B16-F10 cells in Nrf2-null and wild-type mice, respectively (an approximately 20-fold increase in Nrf2-null mice compared with wild-type mice; $p < 0.05$).

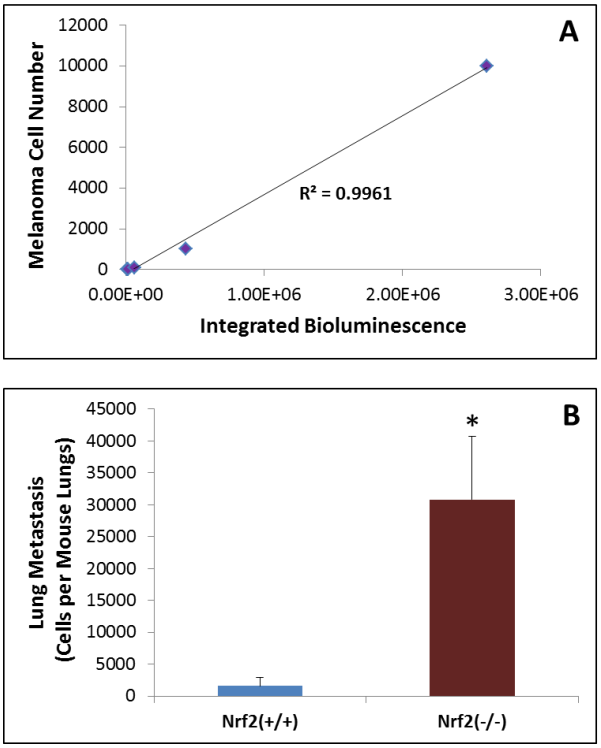

Figure 4. B16-F10 melanoma cell load in the lungs at day 17 in Nrf2-null and wild-type mice following subcutaneous inoculation of B16-F10 cells. Panel A shows a standard curve (a linear correction between bioluminescence intensity and cell number). Data in panel B represent means ± SEM (n = 11 for Nrf2-null group and n = 10 for wild-type group). *, $p < 0.05$ compared with respective wild-type group.

4. DISCUSSION

Nrf2, the chief regulator of cellular antioxidant and phase 2 defenses, is suggested to act as a double-edged sword in cancer development. On the one hand, Nrf2 activation may protect against chemically induced cell initiation, thereby preventing chemical carcinogenesis. On the other hand, by increasing antioxidant defenses and altering cellular redox status, Nrf2 signaling seems to promote tumorigenesis, thus acting as a potential proto-oncogene. In this regard, antioxidants have been shown to promote cancer growth and metastasis in certain animal models [10, 11]. In line with this notion, reactive oxygen species (ROS) or ROS-enhancing chemicals have been shown to be effective in cancer treatment in both animal models and human studies [12–14]. Cancer cells typically produce elevated levels of ROS and also are more susceptible to oxidative stress than normal cells, and this explains, at least partially, why ROS-enhancing agents possess anticancer activity to some extent. Increasing antioxidant defenses via Nrf2 signaling in cancer cells would reduce cellular ROS levels, thus providing a more favorable environment for cancer cell proliferation. Although this notion is conceptually sound, the exact role of Nrf2 signaling in tumorigenesis remains controversial and different studies yielded different, if not opposite, conclusions. Hence, additional studies under various conditions are warranted to further understand the complexity of the Nrf2-tumorigenesis phenomenon.

This study aimed to investigate the role of Nrf2 signaling in influencing melanoma growth and lung metastasis using Nrf2-null mice. Melanoma is one of the most metastatic cancers, and B16-F10 melanoma cell line has been widely used to study melanoma growth and metastasis in animal models [15–18]. In this regard, intravenous inoculation of B16-F10 cells is a commonly used approach to creating lung metastasis in C57BL/6 mice [15–18]. However, this procedure does not mimic the natural metastasis of melanoma from the skin to distant organs, including the lungs. Hence, in this study, we investigated the impact of Nrf2 status on the growth and lung metastasis of B16-F10 cells following subcutaneous injection of the cancer cells.

We also applied a recently developed highly sensitive bioluminometric assay [9] to determine lung metastasis by quantifying the melanoma cell load in mouse lungs following subcutaneous inoculation. Our results demonstrated for the first time that Nrf2 deficiency significantly promoted the growth of subcutaneously inoculated B16-F10 cells as indicated by increased proportion of animals with locally palpable tumor mass and time-dependent increases in tumor volume at the injection site. In vivo bioluminescence imaging also revealed increased growth of melanoma in Nrf2-null mice compared with wild-type mice. Notably, Nrf2 deficiency resulted in a ~20-fold increase in melanoma cell load in the lungs as compared to the wild type genotype.

It remains unclear why Nrf2 deficiency promotes melanoma growth and lung metastasis. A possible mechanism could be related to the dysregulated im-

munity in Nrf2-null mice [19]. In this context, growth and metastasis of melanoma are particularly influenced by the immunity of the host. Indeed, immunotherapy with antibody blockage of CTLA-4 (an inhibitor of T cell immunity) or PD-1 (a checkpoint protein on T cells) has recently emerged as a promising strategy for treating advanced melanoma in humans [20–22]. As indicated earlier, a role for Nrf2 in modulating immunity has been reported in early studies [19]. A more recent study suggested that Nrf2 activation enhanced anticancer immunity [23], which might explain why Nrf2 deficiency promoted the growth and metastasis of melanoma, a type of cancer that is heavily influenced by the immune status of the host.

In summary, results of this short communication contribute to our current understanding of the complex role Nrf2 plays in influencing the susceptibility to tumorigenesis. Studies are currently underway to investigate the impact of pharmacological activation of Nrf2 signaling on melanoma growth and metastasis and the involvement of Nrf2-regulated immunity in the process.

ACKNOWLEDGMENTS

The work was supported in part by a grant from the U.S. National Institutes of Health/National Cancer Institute (CA192936) and an investigator-initiated grant (IIG) (09A084) from the American Institute for Cancer Research (AICR).

REFERENCES

1. Ramos-Gomez M, Kwak MK, Dolan PM, Itoh K, Yamamoto M, Talalay P, et al. Sensitivity to carcinogenesis is increased and chemoprotective efficacy of enzyme inducers is lost in Nrf2 transcription factor-deficient mice. *Proc Natl Acad Sci USA* 2001; 98(6):3410–5. doi: 10.1073/pnas.051618798.
2. Aoki Y, Hashimoto AH, Amanuma K, Matsumoto M, Hiyoshi K, Takano H, et al. Enhanced spontaneous and benzo(a)pyrene-induced mutations in the lung of Nrf2-deficient gpt delta mice. *Cancer Res* 2007; 67(12):5643–8. doi: 10.1158/0008-5472.CAN-06-3355.
3. Iida K, Itoh K, Kumagai Y, Oyasu R, Hattori K, Kawai K, et al. Nrf2 is essential for the chemopreventive efficacy of oltipraz against urinary bladder carcinogenesis. *Cancer Res* 2004; 64(18):6424–31. doi: 10.1158/0008-5472.CAN-04-1906.
4. Ohta T, Iijima K, Miyamoto M, Nakahara I, Tanaka H, Ohtsuji M, et al. Loss of Keap1 function activates Nrf2 and provides advantages for lung cancer cell growth. *Cancer Res* 2008; 68(5):1303–9. doi: 10.1158/0008-5472.CAN-07-5003.
5. Inami Y, Waguri S, Sakamoto A, Kouno T, Nakada K, Hino O, et al. Persistent activation of Nrf2 through p62 in hepatocellular carcinoma cells. *J Cell Biol* 2011; 193(2):275–84. doi: 10.1083/jcb.201102031.
6. Wang H, Liu X, Long M, Huang Y, Zhang L, Zhang R, et al. NRF2 activation by antioxidant antidiabetic agents accelerates tumor metastasis. *Sci Transl Med* 2016; 8(334):334ra51. doi: 10.1126/scitranslmed.aad6095.
7. Bauer AK, Cho HY, Miller-Degraff L, Walker C, Helms K, Fostel J, et al. Targeted deletion of Nrf2 reduces urethane-induced lung tumor development in mice. *PLoS One* 2011; 6(10):e26590. doi: 10.1371/journal.pone.0026590.
8. Cheung KL, Lee JH, Khor TO, Wu TY, Li GX, Chan J, et al. Nrf2 knockout enhances intestinal tumorigenesis in $Apc^{min/+}$ mice due to attenuation of anti-oxidative stress pathway while potentiates inflammation. *Mol Carcinog* 2014; 53(1):77–84. doi: 10.1002/mc.21950.
9. Zhu H, Kauffman ME, Li JZ, Sarkar S, Trush MA, Jia Z, et al. Innovative bioluminometric quantification of cancer cell load in target organs: implications for studying anticancer drugs, including ROS enhancers. *Reactive Oxygen Species* 2016; 1(2):157-64. doi:10.20455/ros.2016.819.
10. Piskounova E, Agathocleous M, Murphy MM, Hu Z, Huddlestun SE, Zhao Z, et al. Oxidative stress inhibits distant metastasis by human melanoma cells. *Nature* 2015; 527(7577):186–91. doi: 10.1038/nature15726.
11. Hopkins RZ. ROS in Cell 2015. *Reactive Oxygen Species* 2016; 2(4) (in press). doi: 10.20455/ros.2016.849.
12. Anderson CP, Matthay KK, Perentesis JP, Neglia JP, Bailey HH, Villablanca JG, et al. Pilot study of intravenous melphalan combined with continuous infusion L-S,R-buthionine sulfoximine for children with recurrent neuroblastoma. *Pediatr Blood Cancer* 2015; 62(10):1739–46. doi: 10.1002/pbc.25594.

13. Kasiappan R, Safe SH. ROS-inducing agents for cancer chemotherapy. *Reactive Oxygen Species* 2016; 1(1):22-37. doi: 10.20455/ros.2016.805.
14. Li YR. Vitamin C, a multi-tasking molecule, finds a molecular target in killing cancer cells. *Reactive Oxygen Species* 2016; 1(2):141-156. doi: 10.20455/ros.2016.829
15. Okoye I, Wang L, Pallmer K, Richter K, Ichimura T, Haas R, et al. T cell metabolism. The protein LEM promotes $CD8^+$ T cell immunity through effects on mitochondrial respiration. *Science* 2015; 348(6238):995–1001. doi: 10.1126/science.aaa7516.
16. Tan AS, Baty JW, Dong LF, Bezawork-Geleta A, Endaya B, Goodwin J, et al. Mitochondrial genome acquisition restores respiratory function and tumorigenic potential of cancer cells without mitochondrial DNA. *Cell Metab* 2015; 21(1):81–94. doi: 10.1016/j.cmet.2014.12.003.
17. Kreiter S, Vormehr M, van de Roemer N, Diken M, Lower M, Diekmann J, et al. Mutant MHC class II epitopes drive therapeutic immune responses to cancer. *Nature* 2015; 520(7549):692–6. doi: 10.1038/nature14426.
18. Peinado H, Aleckovic M, Lavotshkin S, Matei I, Costa-Silva B, Moreno-Bueno G, et al. Melanoma exosomes educate bone marrow progenitor cells toward a pro-metastatic phenotype through MET. *Nat Med* 2012; 18(6):883–91. doi: 10.1038/nm.2753.
19. Aw Yeang HX, Hamdam JM, Al-Huseini LM, Sethu S, Djouhri L, Walsh J, et al. Loss of transcription factor nuclear factor-erythroid 2 (NF-E2) p45-related factor-2 (Nrf2) leads to dysregulation of immune functions, redox homeostasis, and intracellular signaling in dendritic cells. *J Biol Chem* 2012; 287(13):10556–64. doi: 10.1074/jbc.M111.322420.
20. Couzin-Frankel J. Breakthrough of the year 2013. Cancer immunotherapy. *Science* 2013; 342(6165):1432–3. doi: 10.1126/science.342.6165.1432.
21. Robert C, Long GV, Brady B, Dutriaux C, Maio M, Mortier L, et al. Nivolumab in previously untreated melanoma without BRAF mutation. *N Engl J Med* 2015; 372(4):320–30. doi: 10.1056/NEJMoa1412082.
22. Chapman PB, D'Angelo SP, Wolchok JD. Rapid eradication of a bulky melanoma mass with one dose of immunotherapy. *N Engl J Med* 2015; 372(21):2073–4. doi: 10.1056/NEJMc1501894.
23. Satoh H, Moriguchi T, Saigusa D, Baird L, Yu L, Rokutan H, et al. NRF2 intensifies host defense systems to prevent lung carcinogenesis, but after tumor initiation accelerates malignant cell growth. *Cancer Res* 2016. doi: 10.1158/0008-5472.CAN-15-1584.